



HAL
open science

Exact zero transmission during the Fano resonance phenomenon in non symmetric waveguides

Lucas Chesnel, Sergei A Nazarov

► **To cite this version:**

Lucas Chesnel, Sergei A Nazarov. Exact zero transmission during the Fano resonance phenomenon in non symmetric waveguides. *Zeitschrift für Angewandte Mathematik und Physik*, 2020. hal-02189311v2

HAL Id: hal-02189311

<https://hal.science/hal-02189311v2>

Submitted on 21 Dec 2020

HAL is a multi-disciplinary open access archive for the deposit and dissemination of scientific research documents, whether they are published or not. The documents may come from teaching and research institutions in France or abroad, or from public or private research centers.

L'archive ouverte pluridisciplinaire **HAL**, est destinée au dépôt et à la diffusion de documents scientifiques de niveau recherche, publiés ou non, émanant des établissements d'enseignement et de recherche français ou étrangers, des laboratoires publics ou privés.

Exact zero transmission during the Fano resonance phenomenon in non symmetric waveguides

LUCAS CHESNEL¹, SERGEI A. NAZAROV²

¹ INRIA/Centre de mathématiques appliquées, École Polytechnique, Université Paris-Saclay, Route de Saclay, 91128 Palaiseau, France;

² St. Petersburg State University, Universitetskaya naberezhnaya, 7-9, 199034, St. Petersburg, Russia;

E-mails: lucas.chesnel@inria.fr, srgnazarov@yahoo.co.uk, s.nazarov@spbu.ru

(April 4, 2020)

Abstract. We investigate a time-harmonic wave problem in a waveguide. We work at low frequency so that only one mode can propagate. It is known that the scattering matrix exhibits a rapid variation for real frequencies in a vicinity of a complex resonance located close to the real axis. This is the so-called Fano resonance phenomenon. And when the geometry presents certain properties of symmetry, there are two different real frequencies such that we have either $R = 0$ or $T = 0$, where R and T denote the reflection and transmission coefficients. In this work, we prove that without the assumption of symmetry of the geometry, quite surprisingly, there is always one real frequency for which we have $T = 0$. In this situation, all the energy sent in the waveguide is backscattered. However in general, we do not have $R = 0$ in the process. We provide numerical results to illustrate our theorems.

Key words. Waveguides, Fano resonance, zero transmission, scattering matrix.

1 Introduction

The Fano resonance is a universal phenomenon in physics which appears in many areas. For a general presentation, we refer the reader to [18] for the seminal paper and to [27, 26] for recent reviews. In this work, we consider its expression on a model problem of propagation of time-harmonic waves in a waveguide, which is unbounded in one direction. This problem appears naturally for instance in acoustics, in water-waves theory or in electromagnetism. In this context, the Fano resonance mechanism can be described as follows. Assume that the Neumann Laplacian (for the problem we consider below) has a real eigenvalue λ^0 embedded in the continuous spectrum. In this case, the corresponding eigenfunctions are the so-called trapped modes which are exponentially decaying at infinity. Then perturbing slightly the setting, for example the geometry or the material index, in general this real eigenvalue will turn into a complex resonance [2, 45, 36]. And for real spectral parameters λ (proportional to the square of the frequency) varying in a neighbourhood of λ^0 , the scattering matrix will exhibit a rapid variation. This variation is even quicker as the imaginary part of the complex resonance is small. When λ^0 is between the first and the second thresholds in the continuous spectrum, so that only two conjugated waves can propagate in the waveguide, the symmetric scattering matrix is composed of two reflection coefficients R , \tilde{R} and one transmission coefficient T (see the notation in (3)). In this case, under certain properties of symmetry of the configuration, one can show that the scattering coefficients take zero values for some real λ around λ^0 . Such particular values for R , \tilde{R} are studied in particular in the context of Perfect Transmission Resonances (PTRs), see e.g. [39, 38, 24, 44, 28]. For the presentation of simple models in optics explaining the Fano resonance phenomenon, we refer the reader to [16, 17]. For more mathematical approaches, one can consult [41, 40, 42, 1, 7]. For computations of complex resonances and numerical investigations of the Fano resonance phenomenon in waveguides, we refer the reader to

[12, 6, 13, 19, 21, 20]. For results concerning the existence of trapped modes associated with eigenvalues embedded in the continuous spectrum, see e.g. [43, 14, 15, 11, 25, 29, 34, 35]. Finally, note that another approach to get rigorously a zero transmission coefficient can be found in [8, 9, 10]. It relies on asymptotic results of the usual scattering matrix in geometries with long branches and is not related to the Fano resonance phenomenon considered in this work.

The goal of this note is to show that without assumption of symmetry of the configuration, the transmission coefficient T still takes the zero value throughout the Fano resonance phenomenon. This was intuited in [23] using a continuation idea from a symmetric setting. In the present work, we prove rigorously the result using a different approach which does not require to start from a symmetric setting. The outline of the article is as follows. First we present the setting in Section 2. Then we perturb the geometry and the frequency of the configuration supporting trapped modes via a small parameter $\varepsilon > 0$ and we recall the results of [7] providing an asymptotic expansion of the scattering matrix with respect to ε tending to zero. In Section 4, we show that miraculously (we have no physical explanation for that), the main asymptotic term in the expansion of the transmission coefficient passes through zero for real λ around λ^0 . Then in Section 5, working as in [10], we demonstrate that the unitary structure of the scattering matrix is enough to deduce that the transmission coefficient itself passes through zero for real λ around λ^0 . We provide some numerical results to illustrate this analysis in Section 6. Finally, we give short concluding remarks. The main result of this work is Theorem 5.1.

2 Setting

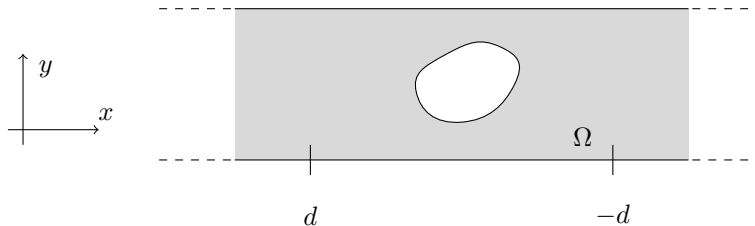


Figure 1: Example of geometry Ω .

Let $\Omega \subset \mathbb{R}^2$ be a domain, that is a connected open set, with Lipschitz boundary $\partial\Omega$ which coincides with the reference strip

$$\{(x, y) \in \mathbb{R} \times (0; 1)\}$$

for $|x| \geq d$ where $d > 0$ is fixed (see Figure 1). We assume that the propagation of time-harmonic waves in Ω is governed by the Helmholtz equation with Neumann boundary conditions

$$\begin{cases} \Delta u + \lambda u = 0 & \text{in } \Omega \\ \partial_\nu u = 0 & \text{on } \partial\Omega. \end{cases} \quad (1)$$

In this problem, u is the quantity of interest (acoustic pressure, velocity potential, component of the electromagnetic field,...), Δ denotes the 2D Laplace operator, λ is a parameter which is proportional to the square of the frequency and ν stands for the normal unit vector to $\partial\Omega$ directed to the exterior of Ω . Note that from time to time, abusively we will call λ the frequency. We emphasize that we consider an academic 2D problem only to simplify the presentation. Other configurations can be dealt with in a completely similar way. In particular, the analysis is the same in higher dimension and in waveguides for which the two unbounded branches are not aligned. Moreover, we can also impose Dirichlet or periodic boundary conditions in (1) to study quantum waveguides or gratings. For $\lambda \in (0; \pi^2)$, only the plane waves w_\pm defined by

$$w_\pm(x, y) = e^{\pm ix\sqrt{\lambda}} \quad (2)$$

can propagate in Ω . For $\lambda \in (0; \pi^2)$, the problem (1) has solutions u_{\pm} admitting the decompositions

$$u_+ = \begin{cases} w_+ + R_+ w_- + \dots, & \text{for } x < -d \\ T w_+ + \dots, & \text{for } x > d, \end{cases} \quad u_- = \begin{cases} T w_- + \dots, & \text{for } x < -d \\ w_- + R_- w_+ + \dots, & \text{for } x > d. \end{cases} \quad (3)$$

Here $R_{\pm} \in \mathbb{C}$ are reflection coefficients and $T \in \mathbb{C}$, which is the same both for u_+ and u_- due to the reciprocity relation, is the transmission coefficient. Moreover, the dots stand for remainders in $H^1(\Omega)$ which decay as $O(e^{-|x|\sqrt{\pi^2-\lambda}})$ when $|x| \rightarrow +\infty$. Physically, u_+ (resp. u_-) models the scattering of the incident rightgoing wave w_+ (resp. leftgoing wave w_-) by the perturbation in the geometry with respect to the reference strip $\mathbb{R} \times (0; 1)$. We define the scattering matrix

$$\mathfrak{s} := \begin{pmatrix} R_+ & T \\ T & R_- \end{pmatrix} \in \mathbb{C}^{2 \times 2}.$$

It is a classical exercise to show that \mathfrak{s} is unitary ($\mathfrak{s}\mathfrak{s}^\top = \text{Id}$) and symmetric ($\mathfrak{s} = \mathfrak{s}^\top$). The functions u_{\pm} are uniquely defined if and only if trapped modes (non-zero solutions of (1) which are in $L^2(\Omega)$) do not exist at the chosen λ . If trapped modes exist, we define uniquely u_{\pm} as the functions admitting the expansions (3) and which are orthogonal to the linear space of trapped modes (which is of finite dimension) in $L^2(\Omega)$.

We assume that the geometry Ω is such that $\lambda = \lambda^0 \in (0; \pi^2)$ is a simple eigenvalue of the Neumann Laplacian. In other words, we assume there is a non zero $u_{\text{tr}} \in L^2(\Omega)$ satisfying $\Delta u_{\text{tr}} + \lambda^0 u_{\text{tr}} = 0$ in Ω , $\partial_\nu u_{\text{tr}} = 0$ on $\partial\Omega$ and that any L^2 solution of (1) is proportional to u_{tr} . Note that since the continuous spectrum of the Neumann Laplacian in Ω is $\sigma_c = [0; +\infty)$, the eigenvalue is embedded in σ_c . To set ideas, we impose that $\|u_{\text{tr}}\|_{L^2(\Omega)} = 1$. Using decomposition in Fourier series, we obtain the expansion

$$u_{\text{tr}} = K e^{-x\sqrt{\pi^2-\lambda^0}} \cos(\pi y) + \tilde{u}_{\text{tr}} \quad \text{for } x \geq d, \quad (4)$$

where K is a constant and \tilde{u}_{tr} is a remainder which decays as $O(e^{-x\sqrt{4\pi^2-\lambda^0}})$ when $x \rightarrow +\infty$. We assume that u_{tr} has a slow decay as $x \rightarrow +\infty$, i.e. $K \neq 0$. In case $K = 0$, the analysis below must be adapted but can be done. Without loss of generality, we can impose that $K > 0$. Note that the choice of making an assumption on the decay of u_{tr} as $x \rightarrow +\infty$ is arbitrary. Considering the change $x \mapsto -x$, the analysis below can be developed completely similarly imposing the behaviour as $x \rightarrow -\infty$.

3 Perturbation of the frequency and of the geometry

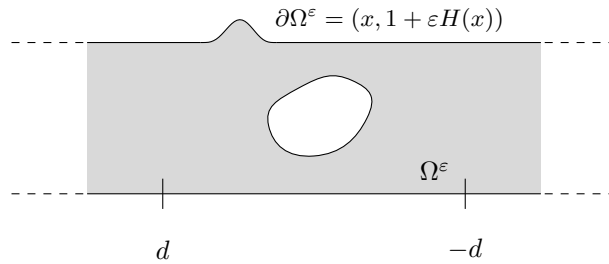


Figure 2: Example of perturbed waveguide Ω^ε .

Now, we perturb slightly the original setting supporting trapped modes. First, the spectral parameter λ^0 is changed for

$$\lambda^\varepsilon = \lambda^0 + \varepsilon \lambda' \quad (5)$$

where $\lambda' \in \mathbb{R}$ is given and $\varepsilon > 0$ is small. Second, we make a perturbation of amplitude ε of the geometry to change Ω into some new waveguide Ω^ε . More precisely, consider $\gamma \subset \partial\Omega$ a smooth

arc. In a neighbourhood \mathcal{V} of γ , we introduce natural curvilinear coordinates (n, s) where n is the oriented distance to γ such that $n > 0$ outside Ω and s is the arc length on γ . Additionally, let $H \in \mathcal{C}_0^\infty(\gamma)$ be a smooth profile function which vanishes in a neighbourhood of the two endpoints of γ . Outside \mathcal{V} , we assume that $\partial\Omega^\varepsilon$ coincides with $\partial\Omega$ and inside \mathcal{V} , $\partial\Omega^\varepsilon$ is defined by the equation

$$n(s) = \varepsilon H(s). \quad (6)$$

In other words if γ is parametrized as $\gamma = \{P(s) \in \mathbb{R}^2 \mid s \in I\}$ where I is a given interval of \mathbb{R} , then $\gamma^\varepsilon := \{P(s) + \varepsilon H(s)\nu(s) \mid s \in I\}$. Here $\nu(s)$ is the unit vector normal to γ at point $P(s)$ directed to the exterior of Ω . Finally we consider the perturbed problem

$$\begin{cases} \Delta u^\varepsilon + \lambda^\varepsilon u^\varepsilon = 0 & \text{in } \Omega^\varepsilon \\ \partial_{\nu^\varepsilon} u^\varepsilon = 0 & \text{on } \partial\Omega^\varepsilon, \end{cases} \quad (7)$$

where ν^ε stands for the normal unit vector to $\partial\Omega^\varepsilon$ directed to the exterior of Ω^ε . We denote by

$$\mathfrak{s}(\varepsilon, \lambda), \quad T(\varepsilon, \lambda), \quad R_+(\varepsilon, \lambda), \quad R_-(\varepsilon, \lambda)$$

the scattering parameters introduced in the previous section in the geometry Ω^ε at frequency λ . And for short, we set

$$\mathfrak{s}^0 := \mathfrak{s}(0, \lambda^0), \quad T^0 := T(0, \lambda^0), \quad R_+^0 := R_+(0, \lambda^0), \quad R_-^0 := R_-(0, \lambda^0).$$

To recall the Theorem 5.1 of [7] describing the behaviour of the scattering matrix $\mathfrak{s}(\varepsilon, \lambda^0 + \varepsilon\lambda')$ as ε goes to zero, and which will be the basis of our analysis below, we need to introduce a few quantities. Set $U := (u_+, u_-)$ where u_\pm are the functions introduced in (3) for $\lambda = \lambda^0$. Set also

$$\kappa(H) := \int_I H(s) (|\partial_s u_{\text{tr}}(0, s)|^2 - \lambda^0 |u_{\text{tr}}(0, s)|^2) ds \in \mathbb{R}, \quad (8)$$

$$\alpha := \int_\Omega u_{\text{tr}}(x, y) \overline{U(x, y)} dx dy \in \mathbb{C} \times \mathbb{C}, \quad (9)$$

$$\beta(H) := \int_I H(s) (\partial_s u_{\text{tr}}(0, s) \overline{\partial_s U(0, s)} - \lambda^0 u_{\text{tr}}(0, s) \overline{U(0, s)}) ds \in \mathbb{C} \times \mathbb{C}. \quad (10)$$

Theorem 3.1. *★ Assume that $\lambda' \neq \kappa(H)$. Then we have*

$$\lim_{\varepsilon \rightarrow 0} \mathfrak{s}(\varepsilon, \lambda^0 + \varepsilon\lambda') = \mathfrak{s}^0.$$

★ Assume that H is such that $\kappa(H)\alpha \neq \beta(H) \in \mathbb{C} \times \mathbb{C}$. Then we have

$$\lim_{\varepsilon \rightarrow 0} \mathfrak{s}(\varepsilon, \lambda^0 + \varepsilon\kappa(H) + \varepsilon^2\mu) = \mathfrak{s}^0 + \frac{\tau^\top \tau}{i\tilde{\mu} - |\tau|^2/2},$$

with $\tau := (\kappa(H)\alpha - \beta(H))\mathfrak{s}$ and $\tilde{\mu} := A\mu + B$ for some unimportant real constants A, B with $A \neq 0$. We emphasize that A, B are independent of ε, μ .

Let us comment this result. To be precise, we should mention that the Theorem 5.1 of [7] is stated in a geometry which is symmetric with respect to the (Oy) axis. Therefore the Theorem 3.1 is a bit different. However the proof is completely similar and is as follows. First, we compute an asymptotic expansion of an auxiliary object called the augmented scattering matrix, which has been introduced in [37, 22] and [30, 32] as $\varepsilon \rightarrow 0$. The essential property is that this augmented scattering matrix considered as a function of (ε, λ) is smooth at $(0, \lambda^0)$. The procedure and the proof of error estimates are detailed in [31, 32, 33]. Then using the relation existing between the usual scattering matrix and the augmented scattering matrix, we can get the statement of the theorem.

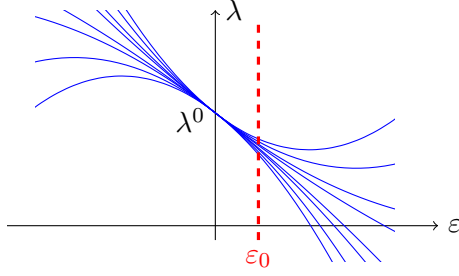


Figure 3: The limit of $\mathfrak{s}(\varepsilon, \lambda^0 + \varepsilon\kappa(H) + \varepsilon^2\mu)$ as $\varepsilon \rightarrow 0$ depends on the parabolic curve chosen for the frequency.

As explained in [7], Theorem 3.1 shows that the scattering matrix $\mathfrak{s}(\cdot, \cdot)$ is not continuous at the point $(0, \lambda^0)$ (setting where trapped modes exist). Indeed, the function $\mathfrak{s}(\cdot, \cdot)$ valued on different parabolic paths $\{(\varepsilon, \lambda^0 + \varepsilon\kappa(H) + \varepsilon^2\mu), \varepsilon \in (0; \varepsilon_0)\}$ (see Figure 3) have different limits when ε tends to zero. And for $\varepsilon_0 \neq 0$ small fixed, the usual scattering matrix $\lambda \mapsto \mathfrak{s}(\varepsilon_0, \lambda)$ exhibits a quick change in a neighbourhood of $\lambda^0 + \varepsilon_0\kappa(H)$. Indeed, the map $\mu \mapsto \mathfrak{s}(\varepsilon_0, \lambda^0 + \varepsilon_0\kappa(H) + \varepsilon_0^2\mu)$ has a large variation for $\mu \in [-C\varepsilon_0^{-1}; C\varepsilon_0^{-1}]$ for some arbitrary $C > 0$ (which is only a small change for λ^{ε_0}). Said differently, a change of order ε of the frequency leads to a change of order one of the scattering matrix. This is nothing but the Fano resonance phenomenon. For a given $C > 0$, outside an interval of length $C\varepsilon_0$ centred at $\lambda^0 + \varepsilon_0\kappa(H)$, $\mathfrak{s}(\varepsilon_0, \cdot)$ is approximately equal to \mathfrak{s}^0 .

Remark 3.1. *When H is such that $\kappa(H)\alpha = \beta(H) \in \mathbb{C} \times \mathbb{C}$, in general a fast Fano resonance phenomenon appears. More precisely, for a given $\varepsilon_0 \neq 0$ small, the variation of $\mathfrak{s}(\varepsilon_0, \cdot)$ of order one occurs on a range of frequencies of length $O(\varepsilon_0^2)$ (instead of $O(\varepsilon_0)$ when $\kappa(H)\alpha \neq \beta(H)$). We write “in general” because we can also show that for well-chosen geometric perturbations, obtained solving a fixed-point problem, no Fano resonance phenomenon happens and the real eigenvalue embedded in the continuous spectrum keeps this property instead of becoming a complex resonance. In particular, this latter result allows one to construct non symmetric waveguides with eigenvalues embedded in the continuous spectrum (see [32, 33]).*

From now, we denote by $\tau_1, \tau_2 \in \mathbb{C}$ the two components of τ , so that $\tau = (\tau_1, \tau_2)$, and we set

$$\begin{aligned} \mathfrak{s}^\varepsilon(\mu) &:= \mathfrak{s}(\varepsilon, \lambda^0 + \varepsilon\kappa(H) + \varepsilon^2\mu) \\ T^\varepsilon(\mu) &:= T(\varepsilon, \lambda^0 + \varepsilon\kappa(H) + \varepsilon^2\mu) \\ R_+^\varepsilon(\mu) &:= R_+(\varepsilon, \lambda^0 + \varepsilon\kappa(H) + \varepsilon^2\mu) \\ R_-^\varepsilon(\mu) &:= R_-(\varepsilon, \lambda^0 + \varepsilon\kappa(H) + \varepsilon^2\mu). \end{aligned}$$

With this notation, the analysis developed in [7] provides the estimate

$$|\mathfrak{s}^\varepsilon(\mu) - s^{\text{asy}}(\mu)| \leq C\varepsilon \quad \text{with} \quad s^{\text{asy}}(\mu) = \mathfrak{s}^0 + \frac{\tau^\top \tau}{i\tilde{\mu} - |\tau|^2/2}, \quad (11)$$

where in (11), for any compact set $I \subset \mathbb{R}$, the constant $C > 0$ can be chosen independent of $\mu \in I$. In particular, we have

$$|T^\varepsilon(\mu) - T^{\text{asy}}(\mu)| \leq C\varepsilon \quad \text{with} \quad T^{\text{asy}}(\mu) = T^0 + \frac{\tau_1 \tau_2}{i\tilde{\mu} - (|\tau_1|^2 + |\tau_2|^2)/2}. \quad (12)$$

In order to prove that we have $T^\varepsilon(\mu) = 0$ for some $\mu \in \mathbb{R}$ for ε small enough, we first show that the map $\mu \mapsto T^{\text{asy}}(\mu)$ vanishes in \mathbb{R} . This is the object of the next section.

4 Asymptotic behaviour of the transmission coefficient

Proposition 4.1. *Assume that $T^0 \neq 0$. Then we have*

$$\{T^{\text{asy}}(\mu), \mu \in \mathbb{R}\} = \mathcal{C}^{\text{asy}} \setminus \{T^0\}$$

where \mathcal{C}^{asy} is a circle passing through T^0 and zero.

Proof. Using the expression (12) for $T^{\text{asy}}(\mu)$ and classical results concerning the Möbius transform, one can show that $\{T^{\text{asy}}(\mu), \mu \in \mathbb{R}\}$ coincides with $\mathcal{C}^{\text{asy}} \setminus \{T^0\}$, where \mathcal{C}^{asy} is a circle passing through T^0 . Let us show that \mathcal{C}^{asy} also passes through zero. From (12), one finds that $T^{\text{asy}}(\mu) = 0$ for some $\mu \in \mathbb{R}$ if and only if there holds

$$\frac{|\tau_1|^2 + |\tau_2|^2}{2} = \Re e \left(\frac{\tau_1 \tau_2}{T^0} \right). \quad (13)$$

In order to establish (13), we need to derive some relations between T^0 and $\tau = (\tau_1, \tau_2)$. To proceed, first we notice that $U = (u_+, u_-)$ satisfies

$$\bar{U} \mathfrak{s}^0 = U. \quad (14)$$

Indeed, the first component of $\bar{U} \mathfrak{s}^0$ is equal to $R_+^0 \bar{u}_+ + T^0 \bar{u}_-$ and using (3), one finds that this function admits the expansion

$$R_+^0 \bar{u}_+ + T^0 \bar{u}_- = \begin{cases} R_+^0 (w_- + \overline{R_+^0} w_+) + T^0 (\overline{T^0} w_+) + \dots, & \text{for } x < -d \\ R_+^0 (\overline{T^0} w_-) + T^0 (w_+ + \overline{R_-^0} w_-) + \dots, & \text{for } x > d. \end{cases}$$

From the unitarity of \mathfrak{s}^0 , we infer that $R_+^0 \bar{u}_+ + T^0 \bar{u}_-$ has the same expansion as u_+ at infinity. Using that u_{\pm} are orthogonal to u_{tr} in $L^2(\Omega)$, we deduce that $R_+^0 \bar{u}_+ + T^0 \bar{u}_- = u_+$. Similarly, we show that $T^0 \bar{u}_+ + R_-^0 \bar{u}_- = u_-$, which allows us to conclude to (14). Now we exploit (14) to establish the identity

$$\bar{\tau} \mathfrak{s}^0 = \tau. \quad (15)$$

From the expressions (8)-(10) of $\kappa(H)$, α , $\beta(H)$ and the properties of \mathfrak{s}^0 , we obtain

$$\bar{\tau} \mathfrak{s}^0 = (\kappa(H) \bar{\alpha} - \overline{\beta(H)}) \bar{\mathfrak{s}}^0 \mathfrak{s}^0 = \kappa(H) \bar{\alpha} - \overline{\beta(H)}.$$

Then replacing U by $\bar{U} \mathfrak{s}^0$ (identity (14)) in $\kappa(H) \bar{\alpha} - \overline{\beta(H)}$, we get $\bar{\tau} \mathfrak{s}^0 = (\kappa(H) \alpha - \beta(H)) \mathfrak{s}^0 = \tau$. This proves (15) or equivalently

$$\begin{cases} R_+^0 \bar{\tau}_1 + T^0 \bar{\tau}_2 = a \\ T^0 \bar{\tau}_1 + R_-^0 \bar{\tau}_2 = b. \end{cases} \quad (16)$$

Finally, we use (16) to establish (13). The unitarity of \mathfrak{s}^0 imposes $R_-^0 = -\overline{R_+^0} T^0 / \overline{T^0}$. Inserting this relation in the second line of (16) gives

$$T^0 \bar{\tau}_1 - \frac{\overline{R_+^0} T^0}{\overline{T^0}} \bar{\tau}_2 = \tau_2. \quad (17)$$

The first line of (16) implies

$$R_+^0 = \frac{\tau_1 - T^0 \bar{\tau}_2}{\bar{\tau}_1}. \quad (18)$$

Inserting (18) in (17) and multiplying by τ_1 leads to

$$T^0 (|\tau_1|^2 + |\tau_2|^2) - \frac{T^0}{\overline{T^0}} \bar{\tau}_1 \tau_2 = \tau_1 \tau_2 \quad \Leftrightarrow \quad |\tau_1|^2 + |\tau_2|^2 = 2 \Re e \left(\frac{\tau_1 \tau_2}{T^0} \right).$$

This is identity (13). □

Remark 4.1. *The reason why \mathcal{C}^{asy} passes through zero is quite mysterious. When Ω , Ω^ε are symmetric with respect to the (Oy) axis, this can be shown quite simply working with half-waveguides problems (see e.g. [7]). But without assumption of symmetry, we cannot provide a physical interpretation of this fact.*

Denote μ_\star the value of μ such that $T^{\text{asy}}(\mu_\star) = 0$ and for $\varepsilon > 0$, define the interval $I^\varepsilon := (\mu_\star - \sqrt{\varepsilon}; \mu_\star + \sqrt{\varepsilon})$. From (12), for $\varepsilon > 0$ small, we know that the curve

$$C^\varepsilon = \{T^\varepsilon(\mu), \mu \in I^\varepsilon\}$$

passes close to zero. It remains to show that C^ε passes exactly through zero for ε small enough.

5 Exact zero transmission

Now, we state and prove the main result of the article. Its proof relies on Proposition 4.1 and an argument presented in [10] (see also [23]).

Theorem 5.1. *Assume that $T^0 \neq 0$. Then there is $\varepsilon_0 > 0$ such that for all $\varepsilon \in (0; \varepsilon_0]$, there exists $\mu \in \mathbb{R}$ (depending on ε) such that $T^\varepsilon(\mu) = 0$.*

Proof. Let us first give the general idea of the proof. Assume by contradiction that for all $\varepsilon > 0$, $\mu \mapsto T^\varepsilon(\mu)$ does not pass through zero in I^ε . Since $\mathfrak{s}^\varepsilon(\mu)$ is unitary, there holds $R_+^\varepsilon(\mu) \overline{T^\varepsilon(\mu)} + T^\varepsilon(\mu) \overline{R_-^\varepsilon(\mu)} = 0$ and so

$$-R_+^\varepsilon(\mu)/\overline{R_-^\varepsilon(\mu)} = T^\varepsilon(\mu)/\overline{T^\varepsilon(\mu)} \quad \forall \mu \in I^\varepsilon. \quad (19)$$

But if $\mu \mapsto T^\varepsilon(\mu)$ does not pass through zero on I^ε , using Proposition 4.1 one can verify that the point $T^\varepsilon(\mu)/\overline{T^\varepsilon(\mu)} = e^{2i \arg(T^\varepsilon(\mu))}$ must run rapidly on the unit circle for $\mu \in I^\varepsilon$ as $\varepsilon \rightarrow 0$. On the other hand, $R_+^\varepsilon(\mu)/\overline{R_-^\varepsilon(\mu)}$ tends to a constant in I^ε as $\varepsilon \rightarrow 0$. This way we obtain a contradiction. We emphasize that the unitary structure of $\mathfrak{s}^\varepsilon(\mu)$ is the key ingredient of this step of the proof. Now we make this discussion more rigorous.

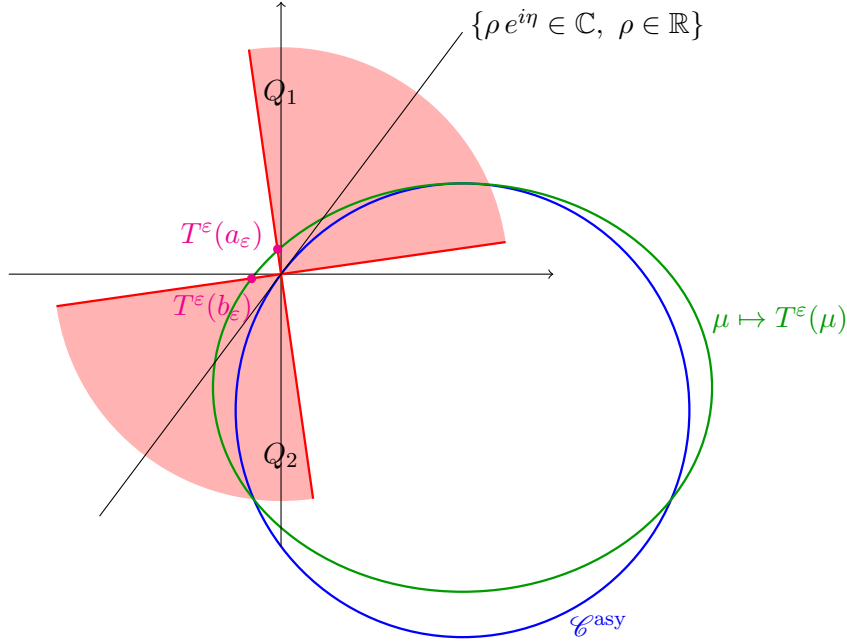


Figure 4: Notation used in the proof of Theorem 5.1.

Since the circle \mathcal{C}^{asy} passes through zero, there is $\eta \in (-\pi/2; \pi/2]$ such that \mathcal{C}^{asy} is tangent to the line $\{\rho e^{i\eta} \in \mathbb{C}, \rho \in \mathbb{R}\}$. Define the quadrants

$$\begin{aligned} Q_1 &:= \{\rho e^{i\theta} \in \mathbb{C} \mid \rho > 0, \eta - \pi/4 < \theta < \eta + \pi/4\} \\ Q_2 &:= \{\rho e^{i\theta} \in \mathbb{C} \mid \rho < 0, \eta - \pi/4 < \theta < \eta + \pi/4\}, \end{aligned}$$

see Figure 4. The graph of the map $\mu \mapsto T^{\text{asy}}(\mu)$ crosses both quadrants Q_1 and Q_2 in I_ε . On the other hand, we have $|T^\varepsilon(\mu) - T^{\text{asy}}(\mu)| \leq C\varepsilon$ where $C > 0$ is independent of $\mu \in I_\varepsilon$ for all $\varepsilon \in (0; \varepsilon_0]$. As a consequence, there is ε_0 such that for all $\varepsilon \in (0; \varepsilon_0]$, the graph of the map $\mu \mapsto T^\varepsilon(\mu)$ intersects both Q_1 and Q_2 on I_ε .

If $\mu \mapsto T^\varepsilon(\mu)$ does not vanish in I^ε , since $\mu \mapsto T^\varepsilon(\mu)$ is continuous, we deduce that for all $\varepsilon \in (0; \varepsilon_0]$,

there are $a_\varepsilon, b_\varepsilon \in I^\varepsilon$ such that $T^\varepsilon(a_\varepsilon) = t_\varepsilon e^{i(\eta-\pi/4)}$ and $T^\varepsilon(b_\varepsilon) = \tilde{t}_\varepsilon e^{i(\eta+\pi/4)}$, with $t_\varepsilon, \tilde{t}_\varepsilon \in \mathbb{R} \setminus \{0\}$. Taking successively $\mu = a_\varepsilon, \mu = b_\varepsilon$ in the relation preceding (19), we obtain

$$R_+^\varepsilon(a_\varepsilon) = -ie^{2i\eta}\overline{R_-^\varepsilon(a_\varepsilon)} \quad \text{and} \quad R_+^\varepsilon(b_\varepsilon) = ie^{2i\eta}\overline{R_-^\varepsilon(b_\varepsilon)}. \quad (20)$$

Introduce the functions R_\pm^{asy} such that

$$R_+^{\text{asy}}(\mu) = R_+^0 + \frac{a^2}{i\tilde{\mu} - (|a|^2 + |b|^2)/2} \quad \text{and} \quad R_-^{\text{asy}}(\mu) = R_-^0 + \frac{b^2}{i\tilde{\mu} - (|a|^2 + |b|^2)/2}.$$

From (11), we know that there is $\varepsilon_0 > 0$ such that, for all $\varepsilon \in (0; \varepsilon_0]$, we have

$$R_+^\varepsilon(a_\varepsilon), R_+^\varepsilon(b_\varepsilon) \in B(R_+^{\text{asy}}(\mu_\star), \varepsilon^{1/4}) \quad \text{and} \quad R_-^\varepsilon(a_\varepsilon), R_-^\varepsilon(b_\varepsilon) \in B(R_-^{\text{asy}}(\mu_\star), \varepsilon^{1/4}),$$

where for $z_0 \in \mathbb{C}$, $B(z_0, r)$ denotes the open disk of \mathbb{C} of radius $r > 0$ centred at z_0 . From (20), we deduce that we must have both

$$B(R_+^{\text{asy}}(\mu_\star), \varepsilon^{1/4}) \cap B(ie^{2i\eta}\overline{R_-^{\text{asy}}(\mu_\star)}, \varepsilon^{1/4}) \neq \emptyset \quad \text{and} \quad B(R_+^{\text{asy}}(\mu_\star), \varepsilon^{1/4}) \cap B(-ie^{2i\eta}\overline{R_-^{\text{asy}}(\mu_\star)}, \varepsilon^{1/4}) \neq \emptyset.$$

This is impossible for ε small enough because $|R_-^{\text{asy}}(\mu_\star)| = 1$ (remember that $T^{\text{asy}}(\mu_\star) = 0$). Thus, we deduce that for all $\varepsilon \in (0; \varepsilon_0]$, $\mu \mapsto T^\varepsilon(\mu)$ cancels in I^ε . \square

Concerning the zeros of $\mu \mapsto R_+^\varepsilon(\mu)$, we can make the following comments. When ε tends to zero, from (11), we know that the curve $\{R_+^\varepsilon(\mu), \mu \in \mathbb{R}\}$ gets closer and closer to $\{R_+^{\text{asy}}(\mu), \mu \in \mathbb{R}\}$. The set $\{R_+^{\text{asy}}(\mu), \mu \in \mathbb{R}\}$ is a circle. It passes through zero if and only if we have

$$\frac{|a|^2 + |b|^2}{2} = \Re e \left(\frac{a^2}{R_+^0} \right). \quad (21)$$

Dividing the first line of (16) by R_+^0 and computing the square of the modulus, we obtain the identity

$$|a|^2 \left(1 + \frac{1}{|R_+^0|^2} \right) - 2 \Re e \left(\frac{a^2}{R_+^0} \right) = \frac{|T^0|^2}{|R_+^0|^2} |b|^2.$$

Using the above equality, we obtain that (21) is satisfied if and only if there holds

$$|a| = |b|. \quad (22)$$

As a consequence, if $|a| \neq |b|$, for ε small enough, $\mu \mapsto R_+^\varepsilon(\mu)$ does not pass through zero. Using the definition of τ in Theorem 3.1, we observe that we have $|a| = |b|$ if Ω and H are symmetric with respect to the (Oy) axis. However, surely it is not necessary to consider symmetric geometries to have (22). But we emphasize that if (22) holds in a non symmetric setting, then we cannot work as in the proof of Theorem 5.1 to get exactly $R_+^\varepsilon(\mu) = 0$ for some $\mu \in \mathbb{R}$. Everything lies in the fact that the identity (19) cannot be exploited similarly for the reflection and the transmission coefficients. Therefore, a priori nothing guarantees that exact zero reflection occurs during the Fano resonance phenomenon in a non symmetric waveguide, even when (22) is satisfied.

6 Numerical results

In this section, we illustrate the results obtained above. In the first series of experiments, we work in the geometry

$$\Omega^\varepsilon := \mathbb{R} \times (0; 1) \setminus ([-0.5; 0.5] \times [0.35 + \varepsilon; 0.65 + \varepsilon] \cup [0; 0.5] \times [0.15 + \varepsilon; 0.85 + \varepsilon])$$

pictured in Figure 5 left. In $\Omega := \Omega^0$ the obstacle is symmetric with respect to the line $\mathbb{R} \times \{1/2\}$. According to the results of the literature (see e.g. [15]), we know that there are trapped modes for



Figure 5: Left: geometry of Ω^ε . Right: real part of a trapped mode for $\varepsilon = 0$ and $\sqrt{\lambda^0} \approx 1.9939$.

certain real frequencies in this geometry. Using Perfectly Matched Layers [4, 3, 5], we find that they exist for $\sqrt{\lambda^0} \approx 1.9939$. Figure 5 right represents such a trapped mode in Ω .

The domain Ω^ε is obtained from Ω by shifting by ε the obstacle along the (Oy) axis. Admittedly, this kind of perturbation is not exactly the one considered in (6). However, since there exists an almost identical mapping from Ω to Ω^ε , results are similar. We emphasize that for $\varepsilon > 0$, Ω^ε has no symmetry property. In Figure 6, we display the values of the complex scattering coefficients $R_+(\varepsilon, \lambda)$, $T(\varepsilon, \lambda)$ appearing in the decomposition (3) of u_+ for $\varepsilon = 0.05$ and for $\sqrt{\lambda} \in (1.97; 2.03)$ (note that this interval contains the value $\sqrt{\lambda^0}$). To proceed, we use a P2 finite element method in a truncated geometry. On the artificial boundary created by the truncation, a Dirichlet-to-Neumann operator with 20 terms serves as a transparent condition. As expected, we observe that $\lambda \mapsto T(\varepsilon, \lambda)$ passes through zero.

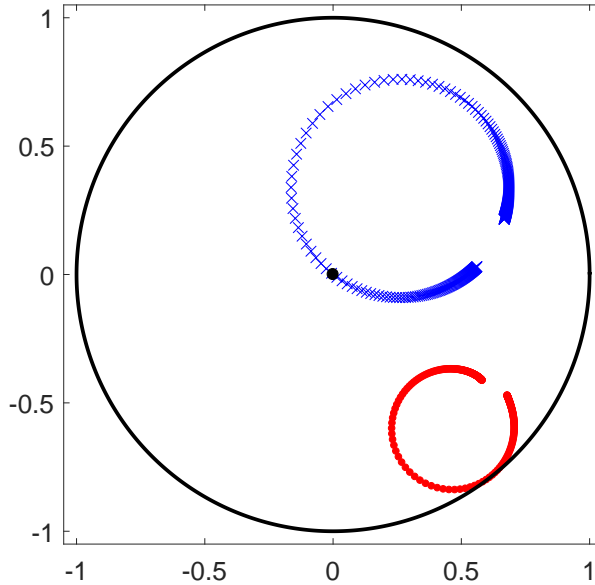


Figure 6: Scattering coefficients $T(\varepsilon, \lambda)$ (\times) and $R_+(\varepsilon, \lambda)$ (\bullet) for $\varepsilon = 0.05$ and $\sqrt{\lambda} \in (1.97; 2.03)$. As predicted, $\lambda \mapsto T(\varepsilon, \lambda)$ passes through zero around λ^0 . According to the conservation of energy, we have $|R_+(\cdot, \cdot)|^2 + |T(\cdot, \cdot)|^2 = 1$ and so the scattering coefficients are located inside the unit disk delimited by the black bold line.

In Figure 7, we display the curves $\lambda \mapsto |T(\varepsilon, \lambda)|$ for several ε and a range of values of λ . The right picture is a zoom of the left picture around λ^0 . As expected we observe that for the different ε , we have $T(\varepsilon, \lambda) = 0$ for one λ close to λ^0 . We also note that the smaller $\varepsilon > 0$ is, the faster the Fano resonance phenomenon occurs. This is also expected. Finally, in Figure 8, we display the real part of u_+ (see (3)) in Ω^ε for $\varepsilon = 0.05$ and $\sqrt{\lambda} = 2.0072$. In this setting, there holds $T(\varepsilon, \lambda) \approx 0$. And indeed we observe that the incident rightgoing wave w_+ is completely backscattered, this is the mirror effect.

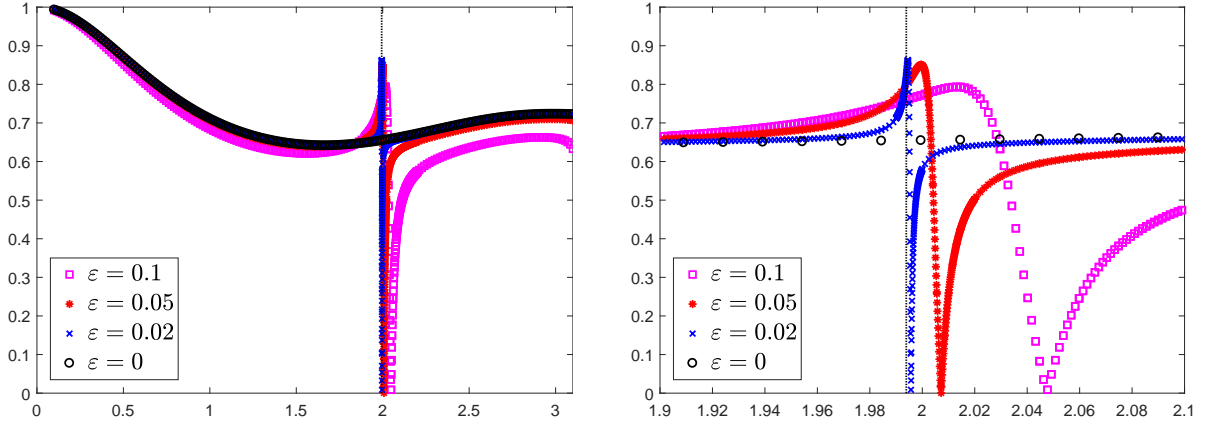


Figure 7: Curves $\lambda \mapsto |T(\varepsilon, \lambda)|$ for several ε and $\sqrt{\lambda} \in (0; \pi)$ (left), $\sqrt{\lambda} \in (1.9; 2.1)$ (right). The vertical dotted line represents the value of $\sqrt{\lambda}^0$.



Figure 8: Real part of u_+ in Ω^ε for $\varepsilon = 0.05$ and $\sqrt{\lambda} = 2.0072$. In this setting, we have $T(\varepsilon, \lambda) \approx 0$.

In the second series of experiments, we work in the geometry of Figure 10. Using Perfectly Matched Layers, we find a complex resonance λ_c such that $\sqrt{\lambda_c} \approx 2.49 - 0.15i$. In Figure 9, we display the values of the complex scattering coefficients $R_+(\lambda)$, $T(\lambda)$ appearing in the decomposition (3) of u_+ for $\sqrt{\lambda} \in (2.1; 2.8)$ (note that this interval contains the value $\Re \sqrt{\lambda_c}$). Though this experiment does not strictly enter the framework presented in this note (we do not start from a situation where trapped modes exist), we observe that the curve $\lambda \mapsto T(\lambda)$ passes through zero for λ in a neighbourhood of $\Re \lambda_c$. In Figure 10, we display the real part of u_+ for $\sqrt{\lambda} = 2.4016$. In this setting, we have $T(\lambda) \approx 0$.

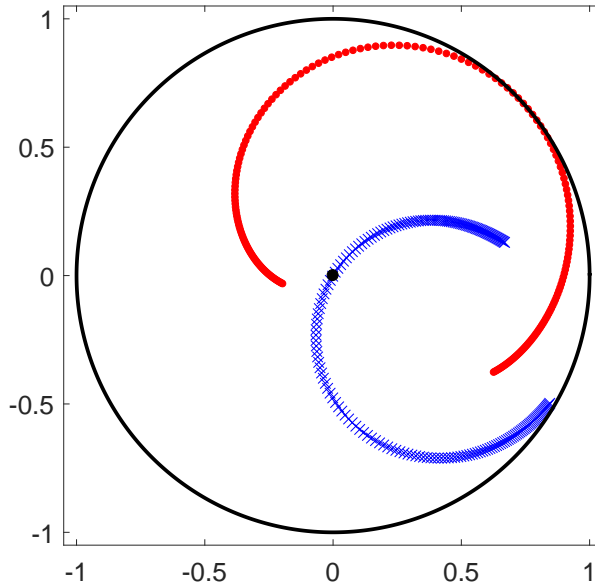


Figure 9: Scattering coefficients $T(\lambda)$ (\times) and $R_+(\lambda)$ (\bullet) for $\sqrt{\lambda} \in (2.1; 2.8)$ in the geometry of Figure 10.

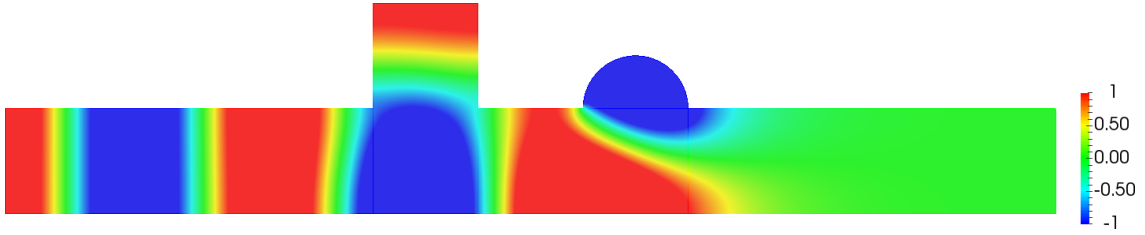


Figure 10: Real part of u_+ for $\sqrt{\lambda} = 2.4016$. In this setting, we have $T(\lambda) \approx 0$.

7 Concluding remarks

In this note, we proved that during the Fano resonance phenomenon in monomode regime, without assumption of symmetry of the geometry, the transmission coefficient passes through zero. Physically, when the transmission coefficient is null, the energy of an incident wave propagating through the structure is completely backscattered. As already mentioned, everything presented here is also valid in higher dimensions and with Dirichlet or periodic boundary conditions instead of Neumann ones. We considered a geometrical perturbation of the walls of the waveguide. We could also have worked with a penetrable inclusion placed in the waveguide. Then perturbing the material parameter, we would have obtained similar results. Importantly, the above analysis applies only in monomode regime, that is for our geometry when λ^0 belongs to $(0; \pi^2)$. It is not clear what happens in multimodal regime ($\lambda^0 > \pi^2$). Moreover, we assumed that λ^0 is a simple eigenvalue embedded in the continuous spectrum of the Neumann Laplacian. When λ^0 is not simple, the analysis has to be done.

Acknowledgments

The research of S.A. Nazarov was supported by the grant No. 17-11-01003 of the Russian Science Foundation.

References

- [1] G.S. Abeynanda and S.P. Shipman. Dynamic resonance in the high-Q and near-monochromatic regime. In *MMET, IEEE*, pages 102–107, 2016.
- [2] A. Aslanyan, L. Parnovski, and D. Vassiliev. Complex resonances in acoustic waveguides. *Quart. J. Mech. Appl. Math.*, 53(3):429–447, 2000.
- [3] E. Bécache, A.-S. Bonnet-Ben Dhia, and G. Legendre. Perfectly matched layers for the convected helmholtz equation. *SIAM J. Numer. Anal.*, 42(1):409–433, 2004.
- [4] J.-P. Berenger. A perfectly matched layer for the absorption of electromagnetic waves. *J. Comput. Phys.*, 114(2):185–200, 1994.
- [5] A.-S. Bonnet-Ben Dhia, L. Chesnel, and V. Pagneux. Trapped modes and reflectionless modes as eigenfunctions of the same spectral problem. *Proc. R. Soc. A*, 474(2213):20180050, 2018.
- [6] G. Cattapan and P. Lotti. Fano resonances in stubbed quantum waveguides with impurities. *Eur. Phys. J. B*, 60(1):51–60, 2007.
- [7] L. Chesnel and S.A. Nazarov. Non reflection and perfect reflection via Fano resonance in waveguides. *Comm. Math. Sci.*, 16(7):1779–1800, 2018.
- [8] L. Chesnel, S.A. Nazarov, and V. Pagneux. Invisibility and perfect reflectivity in waveguides with finite length branches. *SIAM J. Appl. Math.*, 78(4):2176–2199, 2018.
- [9] L. Chesnel and V. Pagneux. Simple examples of perfectly invisible and trapped modes in waveguides. *Quart. J. Mech. Appl. Math.*, 71(3):297–315, 2018.
- [10] L. Chesnel and V. Pagneux. From zero transmission to trapped modes in waveguides. *J. Phys. A: Math. Theor.*, 52(16):165304, 2019.

- [11] E.B. Davies and L. Parnowski. Trapped modes in acoustic waveguides. *Quart. J. Mech. Appl. Math.*, 51(3):477–492, 1998.
- [12] Y. Duan, W. Koch, C.M. Linton, and M. McIver. Complex resonances and trapped modes in ducted domains. *J. Fluid. Mech.*, 571:119–147, 2007.
- [13] E.H. El Boudouti, T. Mrabti, H. Al-Wahsh, B. Djafari-Rouhani, A. Akjouj, and L. Dobrzynski. Transmission gaps and Fano resonances in an acoustic waveguide: analytical model. *J. Phys. Condens. Matter*, 20(25):255212, 2008.
- [14] D.V. Evans. Trapped acoustic modes. *IMA J. Appl. Math.*, 49(1):45–60, 1992.
- [15] D.V. Evans, M. Levitin, and D. Vassiliev. Existence theorems for trapped modes. *J. Fluid. Mech.*, 261:21–31, 1994.
- [16] S. Fan and J.D. Joannopoulos. Analysis of guided resonances in photonic crystal slabs. *Phys. Rev. B*, 65(23):235112, 2002.
- [17] S. Fan, W. Suh, and J.D. Joannopoulos. Temporal coupled-mode theory for the Fano resonance in optical resonators. *J. Opt. Soc. Am. A*, 20(3):569–572, 2003.
- [18] U. Fano. Effects of configuration interaction on intensities and phase shifts. *Physical Review*, 124(6):1866–1878, 1961.
- [19] S. Hein and W. Koch. Acoustic resonances and trapped modes in pipes and tunnels. *J. Fluid. Mech.*, 605:401–428, 2008.
- [20] S. Hein, W. Koch, and L. Nannen. Trapped modes and Fano resonances in two-dimensional acoustical duct–cavity systems. *J. Fluid. Mech.*, 692:257–287, 2012.
- [21] T. Hohage and L. Nannen. Hardy space infinite elements for scattering and resonance problems. *SIAM J. Numer. Anal.*, 47(2):972–996, 2009.
- [22] I.V. Kamotskii and S.A. Nazarov. An augmented scattering matrix and exponentially decreasing solutions of an elliptic problem in a cylindrical domain. *Zap. Nauchn. Sem. S.-Peterburg. Otdel. Mat. Inst. Steklov. (POMI)*, 264(Mat. Vopr. Teor. Rasprostr. Voln. 29):66–82, 2000. (English transl.: *J. Math. Sci.* 2002. V. 111, N 4. P. 3657–3666).
- [23] H.-W. Lee. Generic transmission zeros and in-phase resonances in time-reversal symmetric single channel transport. *Phys. Rev. Lett.*, 82(11):2358, 1999.
- [24] H.-W. Lee and C.S. Kim. Effects of symmetries on single-channel systems: Perfect transmission and reflection. *Phys. Rev. B*, 63(7):075306, 2001.
- [25] C.M. Linton and P. McIver. Embedded trapped modes in water waves and acoustics. *Wave motion*, 45(1):16–29, 2007.
- [26] B. Luk'yanchuk, N.I. Zheludev, S.A. Maier, N.J. Halas, P. Nordlander, H. Giessen, and C.T. Chong. The Fano resonance in plasmonic nanostructures and metamaterials. *Nat. Mater.*, 9(9):707–715, 2010.
- [27] A.E. Miroshnichenko, S. Flach, and Y.S. Kivshar. Fano resonances in nanoscale structures. *Rev. Mod. Phys.*, 82(3):2257, 2010.
- [28] A.E. Miroshnichenko, B.A. Malomed, and Y.S. Kivshar. Nonlinearly PT-symmetric systems: Spontaneous symmetry breaking and transmission resonances. *Phys. Rev. A*, 84(1):012123, 2011.
- [29] S.A. Nazarov. Sufficient conditions on the existence of trapped modes in problems of the linear theory of surface waves. *J. Math. Sci.*, 167(5):713–725, 2010.
- [30] S.A. Nazarov. Asymptotic expansions of eigenvalues in the continuous spectrum of a regularly perturbed quantum waveguide. *Theor. Math. Phys.*, 167(2):606–627, 2011.
- [31] S.A. Nazarov. Eigenvalues of the Laplace operator with the Neumann conditions at regular perturbed walls of a waveguide. *J. Math. Sci.*, 172(4):555–588, 2011.
- [32] S.A. Nazarov. Enforced stability of an eigenvalue in the continuous spectrum of a waveguide with an obstacle. *Comput. Math. and Math. Phys.*, 52(3):448–464, 2012.
- [33] S.A. Nazarov. Enforced stability of a simple eigenvalue in the continuous spectrum of a waveguide. *Funct. Anal. Appl.*, 47(3):195–209, 2013.
- [34] S.A. Nazarov. Gaps and eigenfrequencies in the spectrum of a periodic acoustic waveguide. *Acoust. Phys.*, 59(3):272–280, 2013.
- [35] S.A. Nazarov. Almost standing waves in a periodic waveguide with resonator, and near-

- threshold eigenvalues. *Algebra i Analiz*, 28(3):110–160, 2016. (English transl.: Sb. Math. J. 2017. V. 28, N 3. P. 377–410).
- [36] S.A. Nazarov. Enhancement and smoothing of near-threshold Wood anomalies in an acoustic waveguide. *Acoust. Phys.*, 64(5):535–547, 2018.
- [37] S.A. Nazarov and B.A. Plamenevskiĭ. Selfadjoint elliptic problems: scattering and polarization operators on the edges of the boundary. *Algebra i Analiz*, 6(4):157–186, 1994. (English transl.: Sb. Math. J. 1995. V. 6, N 4. P. 839–863).
- [38] J.A. Porto, F.J. Garcia-Vidal, and J.B. Pendry. Transmission resonances on metallic gratings with very narrow slits. *Phys. Rev. Lett.*, 83(14):2845, 1999.
- [39] Z.-A. Shao, W. Porod, and C.S. Lent. Transmission resonances and zeros in quantum waveguide systems with attached resonators. *Phys. Rev. B*, 49(11):7453, 1994.
- [40] S.P. Shipman and H. Tu. Total resonant transmission and reflection by periodic structures. *SIAM J. Appl. Math.*, 72(1):216–239, 2012.
- [41] S.P. Shipman and S. Venakides. Resonant transmission near nonrobust periodic slab modes. *Phys. Rev. E*, 71(2):026611, 2005.
- [42] S.P. Shipman and A.T. Welters. Resonant electromagnetic scattering in anisotropic layered media. *J. Math. Phys.*, 54(10):103511, 2013.
- [43] F. Ursell. Trapping modes in the theory of surface waves. *Proc. Camb. Philos. Soc.*, 47:347–358, 1951.
- [44] S.V. Zhukovsky. Perfect transmission and highly asymmetric light localization in photonic multilayers. *Phys. Rev. A*, 81(5):053808, 2010.
- [45] M. Zworski. Resonances in physics and geometry. *Not. AMS*, 46(3):319–328, 1999.